

# Global-in-Time Domain Decomposition for a Nonlinear Diffusion Problem

Elyes Ahmed, Caroline Japhet and Michel Kern

## 1 Introduction

We study a simplified model for two-phase flow in porous media, where the medium is made of two (or more) different *rock types*. Each rock type is a subdomain with a distinct capillary pressure function so that the saturation becomes discontinuous across the interface between the different regions. This leads to the phenomenon of capillary trapping (see [12] or [4]).

In this paper we develop a non-overlapping domain decomposition method that combines the Optimized Schwarz Waveform Relaxation method with Robin transmission conditions and the discontinuous Galerkin method in time. The domain decomposition method we present is global-in-time, which provides flexibility for using non-matching time grids so as to handle the very different time scales that occur in the different rocks of the porous medium. The method is a generalization of previous work on linear diffusion or diffusion-advection problems [8, 9].

We state briefly the physical model, referring to [1, 4] for further details. Let  $\Omega$  be a bounded open subset of  $\mathbb{R}^d$  ( $d = 2$  or  $3$ ), assumed to be polygonal, with Lipschitz continuous boundary. We assume that the porous medium  $\Omega$  is heterogeneous and made-up of two rock types, represented by polygonal subsets  $(\Omega_i)_{i \in \{1,2\}}$  (the restriction to two subdomain is only to simplify the exposition, and indeed the example given in section 4 uses more than 2 subdomains). The subdomains share

---

Elyes Ahmed  
Inria, 2 rue Simone iff, 75589 Paris, France,  
current address Department of Mathematics, University of Bergen, P. O. Box 7800, N-5020 Bergen,  
Norway, e-mail: Elyes.Ahmed@uib.no

Caroline Japhet  
Université Paris 13, Sorbonne Paris Cité, LAGA, CNRS(UMR 7539), 93430, Villetaneuse, France,  
e-mail: japhet@math.univ-paris13.fr

Michel Kern  
Inria, 2 rue Simone iff, 75589 Paris, France, e-mail: michel.kern@inria.fr,  
Université Paris-Est, CERMICS (ENPC), 77455 Marne-la-Vallée 2, France.

the interface  $\Gamma = \overline{\Omega}_1 \cap \overline{\Omega}_2$ . We suppose that each subdomain  $\Omega_i$  is homogeneous, in that the physical properties depend on space only through the subdomain index.

We consider the following nonlinear diffusion problem (for some time  $T > 0$ )

$$\partial_t u_i - \nabla \cdot (\lambda_i(u_i) \nabla \pi_i(u_i)) = 0, \quad \text{in } \Omega_i \times (0, T), \quad i = 1, 2, \quad (1)$$

for scalar unknowns  $u_i = u|_{\Omega_i} : \Omega_i \times (0, T) \rightarrow [0, 1]$  representing the gas saturation. This model can be obtained from the complete two-phase flow model by neglecting the advection terms in the saturation equation, so that the saturation and pressure equations become completely decoupled (see [4] for details). In [4], this simplified model is shown to allow gas trapping in low capillary pressure regions. The functions  $\pi_i : [0, 1] \rightarrow \mathbb{R}$  (Lipschitz and strictly increasing) and  $\lambda_i : [0, 1] \rightarrow \mathbb{R}$  are respectively the capillary pressure and the global mobility of the gas in subdomain  $\Omega_i$ . Initial data  $u_0 \in L^2(\Omega)$  is given with  $u_0(x) \in [0, 1]$  for a.e.  $x \in \Omega$ , and for simplicity we assume homogeneous Neumann boundary conditions on  $\partial\Omega$ .

Transmission conditions across the interface  $\Gamma \times [0, T]$  are needed to complement (1). In order to handle the three different cases where both phases can flow across the interface, or where only one phase flows, and the other phase is trapped in a subdomain, one introduces *truncated* capillary pressure curves (see [4] or [1] for details), defined by

$$\bar{\pi}_1(u) = \max(\pi_1(u), \pi_2(0)), \quad \bar{\pi}_2(u) = \min(\pi_2(u), \pi_1(1)).$$

The transmission conditions are then given by

$$\begin{aligned} \bar{\pi}_1(u_1) &= \bar{\pi}_2(u_2) \\ \lambda_1 \nabla \pi_1(u_1) \cdot \mathbf{n}_1 &= -\lambda_2 \nabla \pi_2(u_2) \cdot \mathbf{n}_2 \end{aligned} \quad \text{on } \Gamma \times (0, T), \quad (2)$$

where  $\mathbf{n}_i$  is the unit, outward pointing, normal vector field on  $\partial\Omega_i$ .

In the next section, this physical problem is rewritten in a form better suited for mathematical and numerical analysis. In particular, the existence of a weak solution of the local Robin problems is addressed. A semi-discrete formulation based on discontinuous Galerkin in time is given in section 3 and numerical experiments using a finite volume method are described in section 4.

## 2 Space-time domain decomposition at the continuous level

The model stated above is well adapted to physical modeling, but is difficult to handle mathematically because of the low regularity of the solutions. To obtain mathematical results, it has been found useful to introduce the Kirchhoff transformation [4], so that  $\lambda_i$  and  $\pi_i$  are replaced by a single function  $\varphi_i$ . Following [3, 4], one also introduces new functions  $(\Pi_i)_{i=1,2}$  that satisfy

$$\bar{\pi}_1(u_1) = \bar{\pi}_2(u_2) \Leftrightarrow \Pi_1(u_1) = \Pi_2(u_2), \quad \forall (u_1, u_2) \in [0, 1]^2.$$

Defining the global function  $\Pi_g(x, t) = \Pi_i(u_i(x, t))$ , for  $x \in \Omega_i$ ,  $t \in (0, T)$ , it is shown in the above references that  $\Pi_g(u) \in L^2(0, T; H^1(\Omega))$ , which gives a meaning to the first transmission condition in (4) below.

In terms of the new functions, the problem becomes

$$\partial_t u_i - \Delta \varphi_i(u_i) = 0, \quad \text{in } \Omega_i \times (0, T), \quad u_i(\cdot, 0) = u_0, \quad \text{in } \Omega_i, \quad (3)$$

together with a Neumann boundary condition on  $\partial\Omega_i \setminus \Gamma$  and the transmission conditions

$$\begin{aligned} \Pi_1(u_1) &= \Pi_2(u_2) \\ \nabla \varphi_1(u_1) \cdot \mathbf{n}_1 &= -\nabla \varphi_2(u_2) \cdot \mathbf{n}_2, \end{aligned} \quad \text{on } \Gamma \times (0, T). \quad (4)$$

An existence theorem is known for the transmission problem (3), (4), see [3, 4] where existence of a suitably defined weak solution is proved.

An equivalent formulation to the model problem (3)–(4) can be obtained by replacing (4) with equivalent Robin transmission conditions on  $\Gamma \times (0, T)$ :

$$\begin{aligned} \nabla \varphi_1(u_1) \cdot \mathbf{n}_1 + \alpha_1 \Pi_1(u_1) &= -\nabla \varphi_2(u_2) \cdot \mathbf{n}_2 + \alpha_1 \Pi_2(u_2), \\ \nabla \varphi_2(u_2) \cdot \mathbf{n}_2 + \alpha_2 \Pi_2(u_2) &= -\nabla \varphi_1(u_1) \cdot \mathbf{n}_1 + \alpha_2 \Pi_1(u_1), \end{aligned} \quad \text{on } \Gamma \times (0, T), \quad (5)$$

where  $\alpha_1$  and  $\alpha_2$  are free parameters that can be chosen to enhance the convergence of the method (see [7, 8] for linear problems and [2] for a reaction-diffusion problem with nonlinear source term). It is shown in [1] how the Robin transmission conditions can be extended to Ventcell transmission conditions, to further improve the convergence of the method.

The Optimized Schwarz Waveform Relaxation method with nonlinear Robin transmission conditions (NL–OSWR) is defined by the following iterations for  $k \geq 0$ , where  $\Psi_i^0$  is a given initial Robin guess on  $\Gamma \times (0, T)$  for  $i = 1, 2$ :

$$\begin{aligned} \partial_t u_i^k - \Delta \varphi_i(u_i^k) &= 0, & \text{in } \Omega_i \times (0, T), \\ \nabla \varphi_i(u_i^k) \cdot \mathbf{n}_i + \alpha_i \Pi_i(u_i^k) &= \Psi_i^{k-1}, & \text{on } \Gamma \times (0, T), \end{aligned} \quad (6)$$

with suitable initial and boundary conditions, then set

$$\Psi_i^k := -\nabla \varphi_j(u_j^k) \cdot \mathbf{n}_j + \alpha_i \Pi_j(u_j^k), \quad j = (3 - i), \quad k \geq 1. \quad (7)$$

We give an existence result for the subdomain problem, namely problem (6) with the iteration  $k$  and the subdomain  $\Omega_i$  fixed. Because of the non-linear Robin boundary condition, the result is not standard (references [3] and [4] both assume Neumann boundary conditions). For the rest of this section, we denote by  $\mathcal{O} \subset \mathbb{R}^d$  a polygonal domain with Lipschitz boundary (that plays the role of one the  $\Omega_i$ ), and denote by  $\Gamma$  the part of the boundary of  $\mathcal{O}$  along which the Robin boundary condition applies. First a notion of weak solution is defined:

**Definition 1 (Weak solution for the local Robin problem)**

A function  $u$  is said to be a weak solution of problem (6) (with initial condition  $u_0$  and homogeneous Neumann boundary condition on  $\partial\mathcal{O} \setminus \Gamma$  if it satisfies:

1.  $u \in L^\infty(\mathcal{O} \times (0, T))$ ,  $0 \leq u \leq 1$  for a.e. in  $\mathcal{O} \times (0, T)$ ,
2.  $\varphi(u) \in L^2(0, T; H^1(\mathcal{O}))$ , and  $\Pi(u) \in L^2(0, T; H^1(\mathcal{O}))$ ,
3. For all  $\psi \in C_{\text{test}} = \{h \in H^1(\mathcal{O} \times (0, T)), h(\cdot, T) = 0\}$ ,

$$\begin{aligned}
& - \int_0^T \int_{\mathcal{O}} u(\mathbf{x}, t) \partial_t \psi(\mathbf{x}, t) \, d\mathbf{x} dt - \int_{\mathcal{O}} u_0(\mathbf{x}) \psi(\mathbf{x}, 0) \, d\mathbf{x} \\
& + \int_0^T \int_{\mathcal{O}} \nabla \varphi(u(\mathbf{x}, t)) \cdot \nabla \psi(\mathbf{x}, t) \, d\mathbf{x} dt - \int_0^T \int_{\Gamma} \alpha \Pi(u(\mathbf{x}, t)) \psi \, d\gamma(\mathbf{x}) dt \\
& = \int_0^T \int_{\Gamma} \Psi(\mathbf{x}, t) \psi \, d\gamma(\mathbf{x}) dt, \quad (8)
\end{aligned}$$

where  $d\gamma(\mathbf{x})$  is the  $(d - 1)$ -dimensional Lebesgue measure on  $\partial\mathcal{O}$ .

We then have an existence theorem for the sub-domain problem

**Theorem 1** *Assume that:*

1. the initial condition  $u_0$  is in  $L^\infty(\mathcal{O})$  and satisfies  $u_0(x) \in [0, 1]$  for a.e.  $x \in \mathcal{O}$ ;
2. the right-hand side  $\Psi \in L^2(\mathcal{O} \times (0, T))$ ;
3. the function  $\varphi$  is Lipschitz continuous and strictly increasing on  $(0, 1)$ ;
4. the function  $\Pi$  is continuous and non-decreasing on  $(0, 1)$ ;
5. the Robin coefficient  $\alpha$  is chosen such that:

$$0 < \Psi(x, t) < \alpha \Pi(1), \quad \forall (x, t) \in \mathcal{O} \times (0, T). \quad (9)$$

*Then there exists a weak solution to Problem (6) in the sense of Definition 1.*

The proof is beyond the scope of this article, and will be the topic of a future paper. It is an adaptation to nonlinear Robin boundary conditions of the proof in [3, 4], and is based on the convergence of a finite volume scheme.

Note that in the context of the NL-OSWR method assumption (9) will have to be checked iteratively to prove that the algorithm is well posed (see section 3).

### 3 Semi-discrete space-time domain decomposition with different time steps in the subdomains

We introduce a non-conforming time discretization, that is each subdomain  $\Omega_i$  has its own time discretization, by using a (lowest order) Discontinuous Galerkin (DG) time discretization on each subdomain, together with a projection across the interface (see [7, 8] for an analysis in the linear case). More precisely, for integers  $M_i$ , define  $\delta t_i = T/M_i$ , and denote by  $\mathcal{T}_i$  the partition of  $[0, T]$  in sub-intervals  $J_i^n$  of size  $\delta t_i$ , where  $J_i^n = (t_i^{n-1}, t_i^n]$ , with  $t_i^n = n\delta t_i$ , for  $n = 0, \dots, M_i$ .

For  $i = 1, 2$ , we introduce the space

$$\mathcal{P}_{\mathcal{T}_i}^0 := \{u_i(\cdot, t) : (0, T) \rightarrow L^2(\Gamma); u_i(\cdot, t) \text{ is constant on } J_i^n, 1 \leq n \leq M_i\}.$$

A function in  $\mathcal{P}_{\mathcal{T}_i}^0$  is thus defined by the  $M_i$  functions  $\{u_i^n := u_i(\cdot, t)|_{J_i^n}\}_{1 \leq n \leq M_i}$  in  $L^2(\Gamma)$ . In order to deal with the non-conformity in time, we introduce the  $L^2$  projection operator  $P_{i,j}$  from  $\mathcal{P}_{\mathcal{T}_j}^0(L^2(\Gamma))$  onto  $\mathcal{P}_{\mathcal{T}_i}^0(L^2(\Gamma))$ , i.e., for  $\phi \in \mathcal{P}_{\mathcal{T}_j}^0(L^2(\Gamma))$ ,  $(P_{i,j}\phi)|_{J_i^n}$  is the average value of  $\phi$  on  $J_i^n$ , for  $n = 1, \dots, M_i$ :

$$(P_{i,j}\phi)|_{J_i^n} = \frac{1}{\delta t_i} \sum_{\ell=1}^{M_j} \int_{J_j^\ell \cap J_i^n} \phi.$$

The semi-discrete counterpart in time of the NL-OSWR method (6)–(7) with possibly different time grids in the subdomains can be written as follows:

For  $i = 1, 2$ , given initial iterates  $\Psi_i^0 \in \mathcal{P}_{\mathcal{T}_i}^0$  and starting from the initial condition  $u_i^{0,0} = u_0|_{\Omega_i}$ , a semi-discrete solution  $(u_i^{k,n})_{1 \leq n \leq M_i}$  at step  $k$  of the algorithm is computed by solving, for  $n = 1, \dots, M_i$ ,

$$\begin{aligned} \frac{u_i^{k,n} - u_i^{k,n-1}}{\delta t_i} - \Delta \varphi_i(u_i^{k,n}) &= 0 && \text{in } \Omega_i, \\ \nabla \varphi_i(u_i^{k,n}) \cdot \mathbf{n}_i + \alpha_i \Pi_i(u_i^{k,n}) &= \frac{1}{\delta t_i} \int_{J_i^n} \Psi_i^{k-1}(t) dt, && \text{on } \Gamma \times (0, T). \end{aligned} \quad (10)$$

Then we set

$$\Psi_i^k := P_{i,j} \left( -\nabla \varphi_j(u_j^k(t)) \cdot \mathbf{n}_j + \alpha_i \Pi_j(u_j^k(t)) \right), \quad j = (3-i), k \geq 1. \quad (11)$$

The projections in (11) between arbitrary grids are performed using the algorithm with linear complexity introduced in [5, 6].

Last, we check that the NL-OSWR algorithm is well posed. That is, we need to verify that assumption (9) holds for every iteration. The initial iterate and the Robin coefficients are chosen such that it holds for  $k = 0$ . We have been able to show that this remains true throughout the algorithm only in the case when the capillary pressure functions satisfy

$$\pi_1(0) = \pi_2(0) \text{ and } \pi_1(1) = \pi_2(1).$$

## 4 Numerical experiment

The domain  $\Omega$  is the unit cube, decomposed into two subdomains with two rock types (see figure 1). The mobilities and capillary pressure functions are given by

$$\lambda_{o,i}(u) = u, \quad i \in \{1, 2\}, \quad \pi_1(u) = 5u^2, \quad \text{and} \quad \pi_2(u) = 5u^2 + 1.$$

The initial condition is that the domain contains some quantity of gas, situated only within  $\Omega_1$ , more precisely,  $u_0(\mathbf{x}) = 0.9$  for  $x_1 < 0.4$  and 0 otherwise. The domain is discretized by a mesh of  $20 \times 20 \times 20$  elements, the time discretization is non-conforming, with constant time steps in each subdomain  $\delta t_1 = 10^{-3}$ , and  $\delta t_2 = \frac{1}{8}10^{-2}$ .

The full discretization is carried out with a two-point finite volume scheme [4]. The method is implemented with the Matlab Reservoir Simulation Toolbox [11]. The nonlinear subdomain problem is solved with Newton's method. The only change required to the finite volume scheme to cope with a non-conforming time scheme is the projection of the right hand side of the transmission condition on the grid of the current subdomain, as shown on eq. (11). This is what makes the choice of a DG formalism important, together with a global in time DD method. The resulting scheme is non-conforming in time, and the equivalence with the physical transmission conditions no longer holds.

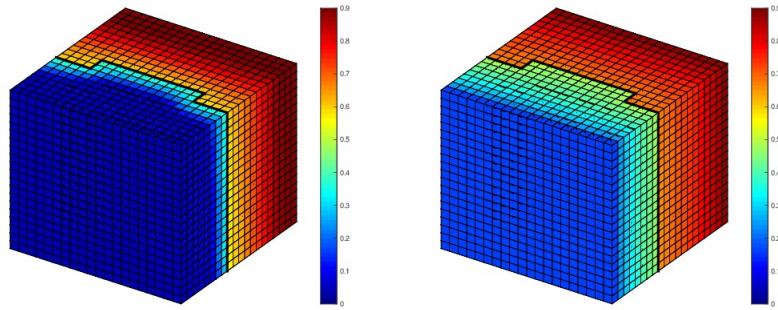
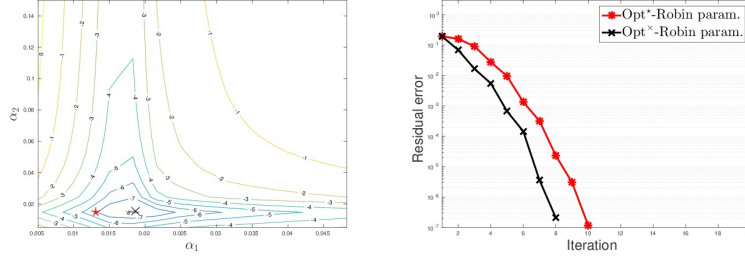


Fig. 1: Test case 1: Saturation  $u(t)$  for  $t = 0.3$  and  $t = 3$

The evolution of the saturation at two time steps is shown in Fig. 1. We remark that at the beginning of the simulation, approximately until  $t \approx 0.02$ , the gas cannot penetrate to the domain  $\Omega_2$ , since the capillary pressure is lower than the threshold value  $\pi_2(0) = 1$ , which is known as the entry pressure. The saturation of the trapped gas in  $\Omega_1$  as well as the capillary pressure increase until the capillary pressure reaches the entry pressure.

We study the convergence behavior of the NL-OSWR algorithm. The tolerance for Newton's method is fixed to  $10^{-8}$ . The tolerance of the NL-OSWR algorithm is  $10^{-6}$ . The Robin parameters are chosen for the two subdomains so as to minimize the convergence rate of a linearized version of the problem. Precisely, we take in the model problem the capillary pressure as unknown, then linearize the nonlinear terms, leading to determine the optimal Robin parameters for a linear diffusion problem with discontinuous coefficients similar to that in [8, 10]. We show in Fig. 2 (right) the relative residuals comparing the convergence history with the parameters calculated numerically by minimizing the convergence factor for the linearized problem and

that of with the best parameters located in the zone giving the smaller errors after the same number of iterations (see Fig. 2 left).



**Fig. 2:** Test case 1: Left: Level curves for the residual error obtained after 10 iterations for various values of the parameters  $\alpha_1$  and  $\alpha_2$ . The star (in magenta) marked the parameters obtained with the minimization process of the convergence factor applied to the linearized problem which is close to the best one marked by times symbol (in black). Right: The convergence curves.

We now analyze the efficiency in time of the method with nonconforming time steps. We compute a reference solution as the converged multidomain solution with conforming fine time grids  $\delta t_f = \frac{1}{4}10^{-3}$ , and where the relative residual is taken smaller than  $10^{-12}$ . We then compare the solution obtained with the nonconforming time steps, as described above with two solutions computed first with conforming fine time steps ( $\delta t_1 = \delta t_2 = 10^{-3}$ ) and then with conforming coarse time steps ( $\delta t_1 = \delta t_2 = \frac{1}{8}10^{-2}$ ). Fig. 3 shows the error in the saturation along a line orthogonal to the interface at three different time steps. One can see that the nonconforming solution as well as the solution with conforming and fine steps are in close agreement with the reference solution, whereas the solution with coarse time steps has a larger error. This confirms that nonconforming time grids with respect to the rock type numerically preserve the accuracy in time of the multidomain solution.

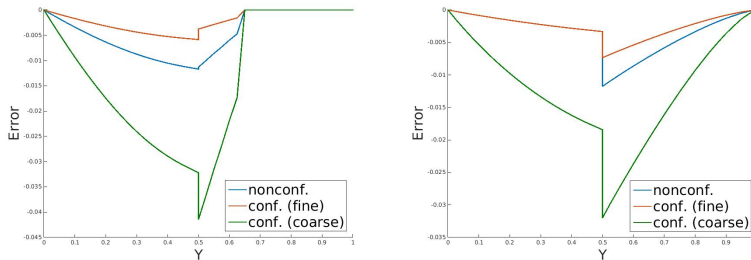


**Fig. 3:** Test case 1. Error in saturation along a line orthogonal to the interface, nonconforming and conforming (coarse and fine) time-steps. Left  $T = T_f / 20$ , right,  $T = T_f$ .

Other examples with more physical content can be found in [1].

**Acknowledgements** This work was funded by ANR DEDALES under grant ANR-14-CE23-0005.

We thank the two referees whose careful comments helped improve the content of the paper.

## References

1. Ahmed, E., Ali Hassan, S., Japhet, C., Kern, M., Vohralík, M.: A posteriori error estimates and stopping criteria for space-time domain decomposition for two-phase flow between different rock types. *The SMAI journal of computational mathematics* **5**, 195–227 (2019). DOI:10.5802/smai-jcm.47. URL [https://smai-jcm.centre-mersenne.org/item/SMAI-JCM\\_2019\\_\\_5\\_\\_195\\_0](https://smai-jcm.centre-mersenne.org/item/SMAI-JCM_2019__5__195_0)
2. Caetano, F., Gander, M.J., Halpern, L., Szeftel, J.: Schwarz waveform relaxation algorithms for semilinear reaction-diffusion equations. *Netw. Heterog. Media* **5**(3), 487–505 (2010). DOI:10.3934/nhm.2010.5.487
3. Cancès, C.: Nonlinear parabolic equations with spatial discontinuities. *NoDEA Nonlinear Differential Equations Appl.* **15**(4-5), 427–456 (2008). DOI:10.1007/s00030-008-6030-7
4. Enchéry, G., Eymard, R., Michel, A.: Numerical approximation of a two-phase flow problem in a porous medium with discontinuous capillary forces. *SIAM J. Numer. Anal.* **43**(6), 2402–2422 (2006). DOI:10.1137/040602936
5. Gander, M.J., Japhet, C.: Algorithm 932: PANG: software for nonmatching grid projections in 2D and 3D with linear complexity. *ACM Trans. Math. Software* **40**(1), Art. 6, 25 (2013). DOI:10.1145/2513109.2513115
6. Gander, M.J., Japhet, C., Maday, Y., Nataf, F.: A new cement to glue nonconforming grids with Robin interface conditions: the finite element case. In: *Domain decomposition methods in science and engineering, Lect. Notes Comput. Sci. Eng.*, vol. 40, pp. 259–266. Springer, Berlin (2005). DOI:10.1007/3-540-26825-1\_24
7. Halpern, L., Japhet, C., Szeftel, J.: Optimized Schwarz waveform relaxation and discontinuous Galerkin time stepping for heterogeneous problems. *SIAM J. Numer. Anal.* **50**(5), 2588–2611 (2012). DOI:10.1137/120865033
8. Hoang, T.T.P., Jaffré, J., Japhet, C., Kern, M., Roberts, J.E.: Space-time domain decomposition methods for diffusion problems in mixed formulations. *SIAM J. Numer. Anal.* **51**(6), 3532–3559 (2013). DOI:10.1137/130914401
9. Hoang, T.T.P., Japhet, C., Kern, M., Roberts, J.E.: Space-time domain decomposition for advection-diffusion problems in mixed formulations. *Math. Comput. Simulation* **137**, 366–389 (2017). DOI:10.1016/j.matcom.2016.11.002
10. Lemarié, F., Debreu, L., Blayo, E.: Toward an optimized global-in-time Schwarz algorithm for diffusion equations with discontinuous and spatially variable coefficients. Part 2: The variable coefficients case. *Electron. Trans. Numer. Anal.* **40**, 170–186 (2013)
11. Lie, K.A., Krogstad, S., Ligaarden, I.S., Natvig, J.R., Nilsen, H.M., Skaflestad, B.: Open source MATLAB implementation of consistent discretisations on complex grids. *Comput. Geosci.* **16**(2), 297–322 (2012). DOI:10.1007/s10596-011-9244-4
12. Van Duijn, C.J., Molenaar, J., De Neef, M.J.: The effect of capillary forces on immiscible two-phase flow in heterogeneous porous media. *Transport in Porous Media* **21**(1), 71–93 (1995). DOI:10.1007/BF00615335